

Interplay between structure and magnetism in $\text{Mo}_{12}\text{S}_9\text{I}_9$ nanowires

Teng Yang,¹ Shinya Okano,¹ Savas Berber,² and David Tománek^{1,*}

¹Physics and Astronomy Department, Michigan State University, East Lansing, Michigan 48824-2320

²Institute of Physics, University of Tsukuba, 1-1-1 Tennodai, Tsukuba, Ibaraki 305-8571, Japan

(Dated: January 8, 2018)

We investigate the equilibrium geometry and electronic structure of $\text{Mo}_{12}\text{S}_9\text{I}_9$ nanowires using *ab initio* Density Functional calculations. The skeleton of these unusually stable nanowires consists of rigid, functionalized Mo octahedra, connected by flexible, bi-stable sulphur bridges. This structural flexibility translates into a capability to stretch up to $\approx 20\%$ at almost no energy cost. The nanowires change from conductors to narrow-gap magnetic semiconductors in one of their structural isomers.

PACS numbers: 81.05.Zx, 61.46.+w, 68.65.-k, 73.22.-f

One of the major challenges in the emerging field of molecular electronics is to identify conducting nanostructures with desired electronic properties, which are stable and easy to manipulate. Due to their high stability and favorable electronic properties [1], carbon nanotubes [2] have been discussed extensively as promising candidates for molecular electronics applications. A major drawback is the current inability to synthesize or to isolate nanotubes with a given diameter and chiral angle, which determine their metallic or semiconducting nature. Moreover, single-wall carbon nanotubes are hard to isolate from stable bundles, which form spontaneously during synthesis [3]. In this respect, recently synthesized nanowires based on Mo chalcogenides, such as $\text{Mo}_{12}\text{S}_9\text{I}_9$, seem to offer several advantages by combining uniform metallic behavior, atomic-scale perfection and easy dispersability [4, 5].

Using *ab initio* density functional calculations, we study the suitability of $\text{Mo}_{12}\text{S}_9\text{I}_9$ nanowires as potential building blocks of electronic nanocircuits. In terms of binding energy per atom, we find these nanowires to be almost as stable as carbon nanotubes. The nanowire skeleton consists of rigid, functionalized Mo octahedra, connected by flexible, bi-stable sulphur bridges. We find this structural flexibility to translate into an unusual capability to stretch up to $\approx 20\%$ at virtually no energy cost, as a nanostructured counterpart of an accordion. Our calculations suggest that the nanowires change from conductors to narrow-gap magnetic semiconductors in one of their structural isomers.

To gain insight into structural and electronic properties of these unusual systems, we optimized the geometry of infinite $\text{Mo}_{12}\text{S}_9\text{I}_9$ nanowires as well as selected structural building blocks using density functional theory (DFT). We used the Perdew-Zunger [6] form of the exchange-correlation functional in the local density approximation (LDA) to DFT, as implemented in the SIESTA code [7]. The behavior of valence electrons was described by norm-conserving Troullier-Martins pseudopotentials [8] with partial core corrections in the Kleinman-Bylander factorized form [9]. We used a double-zeta basis, including initially unoccupied $\text{Mo}5p$ orbitals. We arranged the

nanowires on a tetragonal lattice, with one side of the unit cell given by the lattice constant a . The other sides of the unit cell were taken to be 19.7 \AA long, about twice the nanowire diameter, to limit inter-wire interaction. We sampled the rather short Brillouin zone of these 1D structures by 6 k-points [10]. The charge density and potentials were determined on a real-space grid with a mesh cutoff energy of 150 Ry, which was sufficient to achieve a total energy convergence of better than 2 meV/atom during the self-consistency iterations.

Magnetic ordering in the nanostructures was investigated using the Local Spin Density Approximation (LSDA) within the SIESTA code [7]. Even though LSDA may be considered less rigorous and dependable than LDA, we use it here as a systematic way to estimate net magnetic moments and exchange splitting in 1D nanowires and finite segments of these systems.

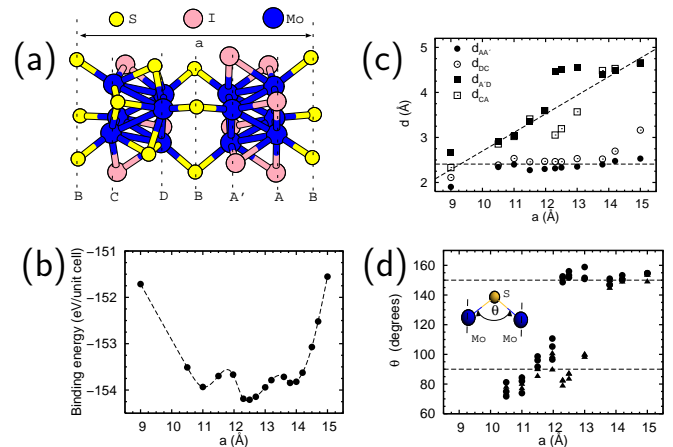


FIG. 1: (Color online) Structural properties of $\text{Mo}_{12}\text{S}_9\text{I}_9$ nanowires. (a) Atomic arrangement within a unit cell. Planes normal to the wire axis are denoted by A, A', B, C, D. (b) Binding energy as a function of the lattice constant a . (c) Optimized inter-plane distances as a function of a . (d) Optimum values of the Mo-S-Mo bond angle Θ as a function of a . Values in the two sulphur bridges per unit cell are distinguished by different symbols. Dashed lines in (b-d) are guides to the eye.

With 30 atoms per unit cell, corresponding to 84 degrees of freedom, global structure optimization is a formidable task. The initial experimental structure determination, based on Atomic-Resolution Transmission Electron Microscopy and X-ray diffraction data [11], provided us with a useful starting point for determining the equilibrium structure. In spite of the significant energy gain of 50 eV with respect to the experimental structure during the initial structure optimization, the calculated atomic arrangement within the $\text{Mo}_{12}\text{S}_9\text{I}_9$ unit cell, depicted in Fig. 1(a), was found to lie very close to the experimental structure.

We found it useful to assign atoms to planes normal to the wire axis. We label these atomic layers A, A', B, C, and D in Fig. 1(a). Layers A and A' are structurally identical in terms of atomic arrangement, but rotated by 180° with respect to each other. Mo octahedra, decorated by S and I atoms, form the structural motif of the AA' and CD bilayers. As we discuss later on, these bilayers can be thought of as rigid blocks, connected by bridges formed of three S atoms, denoted as layer B.

Our results for the binding energy of the system as a function of the lattice constant a are summarized in Fig. 1(b). For lattice constants other than the experimental value [11, 12] $a_{\text{expt}} = 11.97 \text{ \AA}$, the initial structures used in the optimization were based on uniformly expanded or compressed nanowires, subject to random distortions, or structures optimized using semiempirical force fields. We considered a structure as optimized when different starting geometries resulted in the same structural arrangement.

The cohesive energy of the 30-atom unit cell, displayed in Fig. 1(b), translates into a formidable average binding energy exceeding 5 eV per atom. We found that inclusion of $\text{Mo}5p$ orbitals provided a net stabilization of the system, but did not modify much the interatomic forces or equilibrium geometries. As indicated by our LSDA calculations, additional structure stabilization occurred due to magnetic ordering for selected geometries.

Most intriguing in these results is the presence of multiple structural minima. Since structures with optimum lattice constants $a = 11.0 \text{ \AA}$, 12.3 \AA and 13.8 \AA are very close in energy, a distribution of bonding configurations along the chain axis will likely occur in order to maximize configurational entropy, resulting in the loss of long-range order. Identifying structures with very similar energies in a range of lattice constants also implies the possibility to stretch the nanowire by 20% at virtually no energy cost, similar to an accordion. The remarkable ability of $\text{Mo}_6\text{S}_x\text{I}_y$ to expand easily by nearly 30% has been previously noted in Atomic Force Microscope experiments on closely related systems [13]. This uncommon flexibility of an inorganic nanowire may explain in retrospect, why the observed lattice constant [11, 12] $a_{\text{expt}} = 11.97 \text{ \AA}$ may differ from the structural minima in Fig. 1(b).

Trying to understand the origin of the unusual elastic

behavior of $\text{Mo}_{12}\text{S}_9\text{I}_9$ nanowires, we first investigated the inter-layer spacings as a function of the lattice constant. Analysis of our data, presented in Fig. 1(c), suggests that interatomic spacing within AA' and CD bilayers changes very little with increasing lattice constant. The motif of the bilayers is formed of six Mo atoms in near-octahedral arrangement, with Mo-Mo bond lengths close to 2.6 \AA within the layers and 3.0 \AA along the wire axis. In the following, we consider these decorated octahedra as rather rigid building blocks of the nanowires. We found the decoration order by I and S atoms to be non-random, since an interchange of these atoms within the unit cell raised the total energy by more than 0.5 eV.

Most importantly, results in Fig. 1(c) suggested that virtually all structural changes are accommodated by the sulfur bridges, which form the A'-D and C-A connections. We found that most changes occurred in the Mo-S-Mo bond angle Θ , whereas the Mo-S bond lengths remained nearly constant. Our results for Θ as a function of the lattice constant a , shown in Fig. 1(d), suggest that the expectation values of Θ do not change uniformly, but rather group around 90° and 150° . In the following, we will call the corresponding structural arrangements "short" and "long" bridges. Similar metastable structures have also been reported for 1D wires of group IV elements [14]. In the case of isolated sulphur chains and S_3 molecules, we have also observed a preference for similar bond angles as in Fig. 1(d). In analogy with similar preferential bond angles found in different allotropes of C and Si, we associate the short bridge with sp^3 and the long bridge with sp^2 hybridization.

In the case of $\text{Mo}_{12}\text{S}_9\text{I}_9$ nanowires, we find two such sulphur bridges in each unit cell. Local minima in the cohesive energy, plotted in Fig. 1(b), are found at the lattice constants $a = 11.0 \text{ \AA}$, 12.3 \AA , and 13.8 \AA . The fact that only three minima are found, and that $a = 12.3 \text{ \AA}$ is close to the average of the other two lattice constants, supports our conclusion that there are only two types of S-mediated bonds connecting the blocks, which are decoupled within the unit cell. The three local minima in Fig. 1(b) thus correspond to a short-short, short-long (or long-short), and a long-long bridge configuration.

To verify that our optimum structures are not influenced by the constraints of a periodic lattice with a fixed unit cell size, we independently optimized the structure of the Mo-based building blocks with the proper decoration by S and I atoms, with sulphur bridge trimers attached at both sides. With the exception of the bridge atoms, which changed their positions, we found the atomic arrangement in $\text{Mo}_6\text{S}_6\text{I}_6$, modelling the AA' bilayer, and $\text{Mo}_6\text{S}_9\text{I}_3$, modelling the CD bilayer, to lie close to globally optimized nanowire structures, discussed in Fig. 1.

Comparing the binding energies of the bilayer clusters, $E_{\text{coh}}(\text{AA}') = -81.0 \text{ eV}$ and $E_{\text{coh}}(\text{CD}) = -89.2 \text{ eV}$, we conclude that the binding of sulphur atoms to the cluster is significantly stronger than that of iodine atoms. We

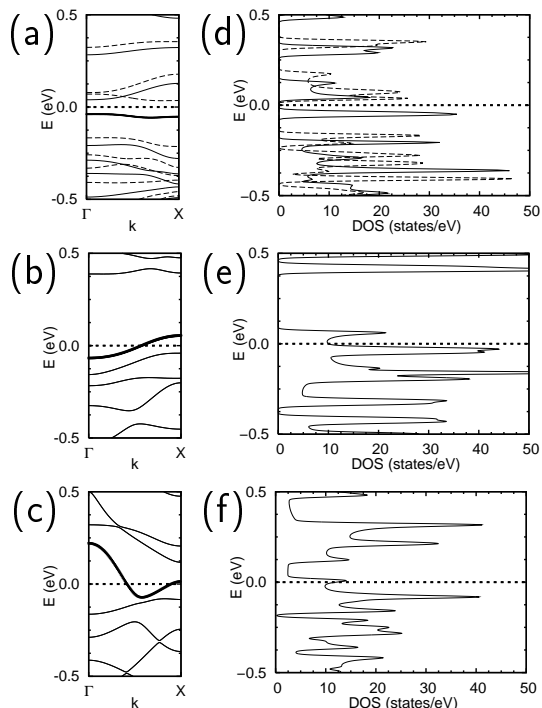


FIG. 2: Electronic band structures $E(k)$ of $\text{Mo}_{12}\text{S}_9\text{I}_9$ nanowires with lattice constants (a) $a = 11.0 \text{ \AA}$, (b) $a = 12.3 \text{ \AA}$, and (c) $a = 13.8 \text{ \AA}$. Solid lines represent majority and dashed lines minority spin bands. Bands crossing the Fermi level are emphasized by heavy lines. Densities of states of nanowires with (d) $a = 11.0 \text{ \AA}$, (e) $a = 12.3 \text{ \AA}$, and (f) $a = 13.8 \text{ \AA}$, convoluted with 0.01 eV wide Gaussians. The Fermi level lies at $E_F = 0$.

also found that the isolated CD cluster acquires a net magnetic moment $\mu(CD) = 1.00 \mu_0$. As we discuss in the following, not only finite nanostructures with dangling bonds, but also infinite nanowires may develop a net magnetic moment.

We found the infinite $\text{Mo}_{12}\text{S}_9\text{I}_9$ nanowires to generally behave as conductors in the lattice constant range $9 \text{ \AA} < a < 15 \text{ \AA}$, with the exception of the metastable structure at $a \approx 11 \text{ \AA}$ discussed below. In Fig. 2 we present results for the electronic structure at $a = 11.0 \text{ \AA}$, 12.3 \AA , and 13.8 \AA , corresponding to the equilibrium structures indicated in Fig. 1(b). The interactions along the nanowire, causing band dispersion, depend crucially on the hybridization near the sulphur bridges. As discussed earlier, changing the lattice constant does not affect interatomic distances, but rather modifies the Mo-S-Mo bond angle Θ , thus changing the hybridization of directional orbitals. An increase in band dispersion, caused by increased hybridization, may be counter-acted by band repulsion in complex systems.

The interplay between lattice constant and band structure is depicted in Figs. 2(a-c). Our results in Figs. 2(b-c) suggest that the metallic character of the wires derives from a rather dispersionless band, which crosses the

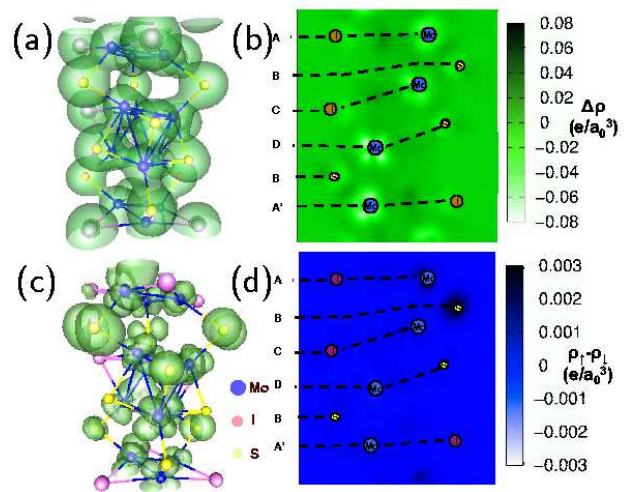


FIG. 3: (Color online) Contour plots depicting the charge distribution in a $\text{Mo}_{12}\text{S}_9\text{I}_9$ nanowire at $a = 11.0 \text{ \AA}$. (a) Total charge density contour at $\rho = 0.05 \text{ el/a}_0^3$. (b) Difference charge density $\Delta\rho(\mathbf{r})$, indicating regions of charge depletion and excess with respect to the superposition of isolated atoms. (c) $\rho = 1.0 \times 10^{-3} \text{ el/a}_0^3$ charge density contour associated with states close to the Fermi level, $E_F - 0.05 \text{ eV} < E < E_F + 0.05 \text{ eV}$. (d) Difference spin density $\rho_{\uparrow}(\mathbf{r}) - \rho_{\downarrow}(\mathbf{r})$, showing regions of excess majority spin \uparrow . Contour plots (b) and (d) are depicted in a plane, which contains the wire axis.

Fermi level. As shown in Fig. 2(a), this band becomes very flat and even changes its slope at $a \approx 11.0 \text{ \AA}$ due to the changed hybridization associated with Mo-S-Mo bond bending. Consequently, the density of states develops a peak at E_F , which subsequently splits due to a magnetic instability, as shown in Fig. 2(d). This splitting opens up a fundamental gap of 73 meV , accompanied by a magnetic moment of $1.00 \mu_0$ per unit cell. At other lattice constants, the dispersion of this partly filled band increases, as seen in Figs. 2(b) and (c). Consequently, as seen in Figs. 2(e) and (f), the density of states at the Fermi level is lower, suppressing the magnetic instability.

A more detailed discussion of the electronic structure in the system with a net magnetic moment, at $a = 11.0 \text{ \AA}$, is presented in Fig. 3. The charge distribution in the $\text{Mo}_{12}\text{S}_9\text{I}_9$ nanowire, depicted in Fig. 3(a), is very similar to the superposition of atomic charge densities. This is better seen in Fig. 3(b), which displays the charge redistribution within the system with respect to isolated atoms, given by $\Delta\rho(\mathbf{r}) = \rho(\mathbf{r}) - \sum \rho_{\text{atom}}(\mathbf{r})$. As expected based on electronegativity differences, we observe a small amount of charge, stemming mostly from Mo $4d$ orbitals, to be transferred to the region within the Mo octahedra, in particular to Mo-Mo bonds and sulphur atoms. The decorating iodine atoms do not experience a change in their charge distribution due to their presence in the nanowire structure. More interesting than information about all populated levels is the spatial distribution of

states close to the Fermi level, which form the valence and conduction band. Our results, shown in Fig. 3(c), suggest that these states are rather delocalized. Together with the band structure results of Fig. 2, we conclude that the nanowires considered here should be conducting at room temperature, in agreement with experimental observations [4, 5].

Spatially resolved information about the magnetic structure of the nanowire at $a = 11.0 \text{ \AA}$ is presented in Fig. 3(d). Associating up-spin with the majority and down-spin with the minority states, the plotted quantity $\rho_{\uparrow}(\mathbf{r}) - \rho_{\downarrow}(\mathbf{r})$ allows us to identify spatial regions with a net magnetic moment. Based on the results in Fig. 3(d) and a set of 3D spin density contours, not shown here, we find the majority spin to be localized mostly on the bridging sulphur atoms, in their non-bonding $2p$ orbitals normal to the wire axis, and to a smaller degree on adjacent Mo atoms.

Since magnetism occurs in selected structural isomers of the infinite $\text{Mo}_{12}\text{S}_9\text{I}_9$ nanowires as well as in isolated building blocks, we expect the possibility of modifying the magnetic structure by locally stretching or expanding the nanowires. Since such structural changes may be induced locally at negligible energy cost, various magnetic patterns could possibly be obtained by mechanical manipulation of $\text{Mo}_{12}\text{S}_9\text{I}_9$ nanowires, possibly using an Atomic Force Microscope. Since magnetic ordering will likely affect spin transport in these systems, $\text{Mo}_{12}\text{S}_9\text{I}_9$ nanowires may be viewed as spin valves, which could change their state by applying local stress.

We note that the overall metallic behavior of $\text{Mo}_{12}\text{S}_9\text{I}_9$ nanowires is rather unusual among chalcogenide structures. Significant interest has been devoted in the past to the ability of layered semiconductors, such as MoS_2 , to form fullerene- and nanotube-like structures [15, 16, 17]. Similar to their bulk counterparts, MoS_2 nanotubes were found to be semiconducting, unless intercalated with iodine to enhance conductance [18, 19]. MoS_2 -based fullerenes and nanotubes, often containing iodine, were noted in particular for their favorable tribological properties [15, 17, 20]. At other stoichiometries, such as $\text{Mo}_6\text{S}_3\text{I}_6$ or $\text{Mo}_6\text{S}_4\text{I}_5$, self-assembled nanowires have been reported to form with either semiconducting or semi-metallic behavior [21, 22]. In the particular $\text{Mo}_{12}\text{S}_9\text{I}_9$ stoichiometry studied here, the rich behavior of molybdenum chalcogenides is complemented by new properties, such as high structural flexibility, metal-semiconductor transition, and magnetism. We propose to use these systems as unique building blocks in hierarchically assembled nanostructured electronic circuits.

We acknowledge discussions and collaboration with Valeria Nicolosi and Jiping Li during the initial stages of this work. Partial funding was provided by the NSF NIRT grants ECS-0103587, ECS-0506309, and NSF NSEC grant EEC-425826.

- [1] R. Saito, G. Dresselhaus, and M. Dresselhaus, *Physical Properties of Carbon Nanotubes* (Imperial College Press, 1998).
- [2] S. Iijima, *Nature* **354**, 56 (1991).
- [3] A. Thess, R. Lee, P. Nikolaev, H. Dai, P. Petit, J. Robert, C. Xu, Y. Lee, S. Kim, D. Colbert, et al., *Science* **273**, 483 (1996).
- [4] V. Nicolosi, D. Vrbancic, A. Mrzel, J. McCauley, S. O'Flaherty, D. Mihailovic, W. J. Blau, and J. N. Coleman, *Chem. Phys. Lett* **401**, 13 (2005).
- [5] V. Nicolosi, D. Vrbancic, A. Mrzel, J. McCauley, S. O'Flaherty, C. McGuinness, G. Compagnini, D. Mihailovic, W. J. Blau, and J. N. Coleman, *J. Phys. Chem. B* **109**, 7124 (2005).
- [6] J. P. Perdew and A. Zunger, *Phys. Rev. B* **23**, 5048 (1981).
- [7] J. M. Soler, E. Artacho, J. D. Gale, A. García, J. Junquera, P. Ordejón, and D. Sánchez-Portal, *J. Phys: Condens. Matter* **14**, 2745 (2002).
- [8] N. Troullier and J. L. Martins, *Phys. Rev. B* **43**, 1993 (1991).
- [9] L. Kleinman and D. M. Bylander, *Phys. Rev. Lett.* **48**, 1425 (1982).
- [10] Details of the electronic structure were obtained using a finer mesh of 16 k-points.
- [11] V. Nicolosi, S. Berber, J. N. Coleman, J. Sloan, D. Tománek, D. Mihailovic, and W. J. Blau, (presentation at the NT'04 conference on the Science and Application of Nanotubes, San Luis Potosí, Mexico, July 19-23, 2004).
- [12] Since the X-ray diffraction peaks in the direction of $\text{Mo}_{12}\text{S}_9\text{I}_9$ nanowires appear somewhat diffuse, we believe that the long-range order, including the lattice constant, is not as well defined as the short range order.
- [13] A. Hassanién, M. Tokumoto, A. Mrzel, D. Mihailovic, and H. Kataura, *Physica E* **29**, 684 (2005).
- [14] R. T. Senger, S. Tongay, E. Durgun, and S. Ciraci, *Phys. Rev. B* **72**, 075419 (2005).
- [15] Y. Feldman, E. Wasserman, D. J. Srolovitz, and R. Tenne, *Science* **267**, 222 (1995).
- [16] G. Seifert, H. Terrones, M. Terrones, G. Jungnickel, and T. Frauenheim, *Phys. Rev. Lett.* **85**, 146 (2000).
- [17] M. Remskar, A. Mrzel, Z. Skraba, A. Jesih, M. Ceh, J. Demšar, P. Stadelmann, F. Lévy, and D. Mihailovic, *Science* **292**, 479 (2001).
- [18] M. Verstraete and J. C. Charlier, *Phys. Rev. B* **68**, 045423 (2003).
- [19] A. Zimina, S. Eisebitt, M. Freiwald, S. Cramm, W. Eberhardt, A. Mrzel, and D. Mihailovic, *Nano Lett.* **4**, 1749 (2004).
- [20] L. Joly-Pottuz, F. Dassenoy, J. Martin, D. Vrbancic, A. Mrzel, D. Mihailovic, W. Vogel, and G. Montagnac, *Tribology Letters* **18**, 385 (2005).
- [21] D. Vrbancic, M. Remskar, A. Jesih, A. Mrzel, P. Umek, M. Ponikvar, B. Jancar, A. Meden, B. Novosel, S. Pejovnik, et al., *Nanotechnology* **15**, 635 (2004).
- [22] A. Meden, A. Kodre, J. P. Gomilsek, I. Arcon, I. Vilfan, D. Vrbancic, A. Mrzel, and D. Mihailovic, *Nanotechnology* **16**, 1578 (2005).

* E-mail: tomanek@msu.edu